Examination of Impedance Response of Capsule-Integrated Antennas Through Gastrointestinal Tract

Erdem Cil*, Sema Dumanli†, and Denys Nikolayev*
*IETR (l'Institut d'électronique et des technologies du numérique) UMR 6164, CNRS / Univ. Rennes, Rennes, France
†Electrical and Electronics Engineering Dept., Bogazici University, Istanbul, Turkey
erdem.cil@univ-rennes1.fr, sema.dumanli@boun.edu.tr, denys.nikolayev@univ-rennes1.fr

***Abstract*—This work focuses on the investigation of the degree of possible detuning that may be observed in the impedance response of ingestible antennas during the transition through the gastrointestinal tract. For this investigation, two fundamental antennas are used: a meandered dipole antenna and a meandered loop antenna. The antennas conform to the inner surface of the biocompatible capsule shell. They are optimized in spherical homogeneous time-averaged gastrointestinal phantoms to operate at 3 different frequencies of interest: 434 MHz, 1.4 GHz, and 2.4 GHz, resulting in 6 different designs in total. Next, the optimized antennas are simulated in 3 different phantoms, each mimicking the electromagnetic properties of one of the tissues in the gastrointestinal tract (stomach, small intestine, and large intestine). The impedance response of each design in 4 different tissues is compared and discussed. The results show that the maximum shift in the operating frequency of the antennas is 7 MHz, indicating that the presence of the encapsulation layer makes the considered antennas robust against the changes in the electromagnetic properties encountered through the gastrointestinal tract.**

***Index Terms*—Capsule antenna, dipole antenna, in-body, ingestible, loop antenna.**

I. Introduction

In recent years, rapid growth has been observed in the use of wireless in-body devices in medical applications. Ingestible devices are one type of these wireless in-body devices. They have a physical structure similar to a capsule and are used by swallowing like conventional pills [1]. Due to their miniature size and compact structure, they are frequently benefited from for various medical purposes such as imaging in a biological system and monitoring diverse physiological parameters inside the human body [1], [2].

Ingestible devices require various components to be integrated into their capsule to operate effectively [3]. Although the design of ingestible devices is multidisciplinary, the ingestible antenna has a key role in the quality of the wireless link formed by these devices. Hence, the ingestible antenna must be designed meticulously so that it is able to meet the requirements of the wireless link in terms of power and efficiency. Various types of antenna designs have been proposed in the literature for ingestible systems such as helix antenna [4], microstrip antenna [5], coil antenna [6], and inverted-F antenna [7].

When a capsule with an ingestible antenna is swallowed, it is transmitted through the gastrointestinal (GI) tract that consists of various tissues, namely the GI tissues, which have different electromagnetic (EM) properties [8]. Therefore, during the design of an in-body antenna, the EM properties of the surrounding environment must be considered, as they strongly affect the antenna parameters such as the operating frequency and antenna efficiency [9]. As the capsule travels through the GI tract, the varying EM properties of different GI tissues may cause a shift in the operating frequency or also affect the antenna efficiency. Thus, an ingestible antenna designer must take into account the changing surrounding environment to ensure the best wireless link quality.

The question one may ask is which antenna parameters must be prioritized while designing an ingestible antenna. For instance, it can be asked whether the designer should concentrate more on the methods to increase antenna efficiency as in [10] or it is more essential to increase the robustness against the changes in the environment. To address this question, the work presented in this paper focuses on the degree of the possible detuning in the operating frequency of ingestible antennas that may result from the varying EM properties of the GI tissues. With this investigation, the paper aims to determine whether robustness against the EM changes in the GI tract must be a priority for ingestible antenna designers. To investigate the degree of detuning, a numerical model that consists of a spherical homogeneous phantom and two different types of antennas (dipole and loop) that are integrated into a capsule is prepared as shown in Fig 1. The antennas are designed to operate at 434 MHz, 1.4 GHz, and 2.4 GHz inside time-averaged GI phantoms, resulting in 6 antenna designs in total. These frequencies are selected for the examination since they are among the most used frequencies in biomedical in-body applications [11]. Next, the optimized antennas are simulated in 3 different phantoms that imitate the EM properties of one of the GI tissues (stomach, small intestine, or large intestine) to observe the degree of the shift in the operating frequency.

This paper is organized as follows. In Section II, the method used for the calculation of the EM properties of time-averaged GI phantoms is explained. In Section III, the antenna models are given. In Section IV, the results are shared and discussed. Finally, the paper concludes in Section V.

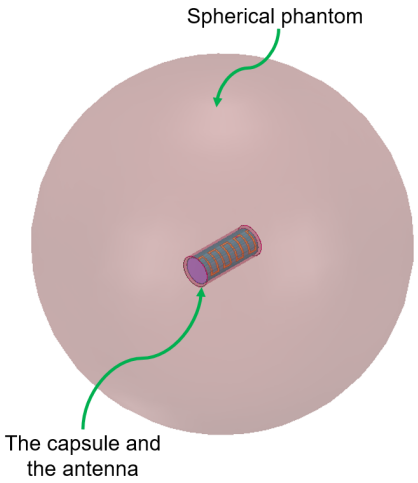

Fig. 1. The numerical model prepared to investigate the degree of the detuning in the operating frequency through the GI tract. The capsule has a length of 20 mm and a diameter of 8.8 mm and the phantom has a diameter of 100 mm.

II. Calculation of EM Properties of Time-Averaged GI Phantoms

To investigate the degree of detuning during the transmission through different GI tissues, the operation of the antennas must be first optimized in a phantom with specific EM properties. One phantom that can be used for the optimization is a phantom that has time-averaged EM properties of the GI tract [12]. To form such a phantom, the time-averaged EM properties are calculated using the time that the capsule spends in each of the tissues. The transition time values are taken from [13]. The EM properties of the GI tissues at 3 frequencies of interest are tabulated in Table I along with the calculated time-averaged values [14]. For instance, the time-averaged relative permittivity is calculated as

$$\frac{180 \times 67.2 + 228 \times 65.3 + 1302 \times 62}{180 + 228 + 1302} = 63 \qquad (1)$$

and the time-averaged conductivity (S/m) is calculated as

$$\frac{180 \times 1.01 + 228 \times 1.92 + 1302 \times 0.87}{180 + 228 + 1302} = 1.02 \qquad (2)$$

at 434 MHz following this approach. Note that the oesophagus is not taken into account during the calculation, as the transit time from the oesophagus to the stomach is only a few seconds, which is negligible.

III. The Capsule and the Antenna Models

The investigation of the degree of detuning is performed using two simple antenna models (a dipole antenna and a loop antenna) for 3 different frequencies (434 MHz, 1.4 GHz, and 2.4 GHz), resulting in 6 different designs in total. Each antenna is integrated into a capsule. The capsule is based on the capsule given in [15] and consists of a 50 μm thick polyimide (PI) substrate (ε_r = 3.4, δ = 0.002) that is wrapped around a cylinder of epoxy-resin (ε_r = 3.1, δ = 0.0037), and a 0.6 mm thick Polyvinyl chloride (PVC) layer (ε_r = 2.6, δ = 0.003) that covers the PI substrate and the epoxy-resin as shown in Fig 2a. The dipole and loop antenna models are shown in Fig. 2b and in Fig. 2c, respectively, along with the parametrized dimensions. The antennas are meandered on the outer surface of the PI substrate. Meandering is required to fit the physically long antennas into the capsule. The capsules are placed in the center of a spherical homogeneous time-averaged GI phantom (explained in Section II) with a radius of 50 mm as visualized in Fig. 1. In each case, the dimensions of the antennas are optimized through numerical analysis using ANSYS High Frequency Structure Simulator (HFSS) [16] to adjust the operating frequency to the corresponding frequency of interest. The final values for the parametrized dimensions are tabulated in Table II. Note that N shows the number of turns for the dipole antenna and the number of sub-loops for the loop antenna as shown in Fig. 2 [17]. It can also be noted that the dipole antennas for 434 MHz and 1.4 GHz are offset-fed dipole antennas. Although a center-fed dipole conventionally exhibits a good impedance matching, the offset-feeding is required in these cases to match the antenna to 50 Ω due to long antenna meandering.

TABLE I
EM Properties of the Tissues in the GI Tract at 3 Frequencies of Interest and Calculated Time-Averaged Values

	Tissue			
	Stomach	Small Intestine	Large Intestine	Average
Transition Time (min)	180	228	1302	*
f = 434 MHz				
Relative Permittivity	67.2	65.3	62	63
Conductivity (S/m)	1.01	1.92	0.87	1.02
f = 1.4 GHz				
Relative Permittivity	63.9	57.1	56.1	57.1
Conductivity (S/m)	1.44	2.44	1.34	1.5
f = 2.4 GHz				
Relative Permittivity	62.2	54.5	54	54.9
Conductivity (S/m)	2.17	3.13	2	2.17

TABLE II
Optimized Values of Parametrized Dimensions at 3 Different Frequencies of Interest

Antenna Model	Frequency (MHz)	Length (mm)	Width (mm)	Trace Width (mm)	Feed Offset (mm)	N
Dipole	434	1.76	18.34	0.5	6.3	7
	1400	2.8	6		5	4
	2400	6.1	3.95		0	2
Loop	434	9.1	0.83	0.3	0	22
	1400	7.25	2.3			4
	2400	5.25	1.57			4

IV. Results and Discussion

Each antenna optimized in Section III is simulated in 3 phantoms that mimic the EM properties of one of the 3 GI tissues at the corresponding frequency: the stomach, the small

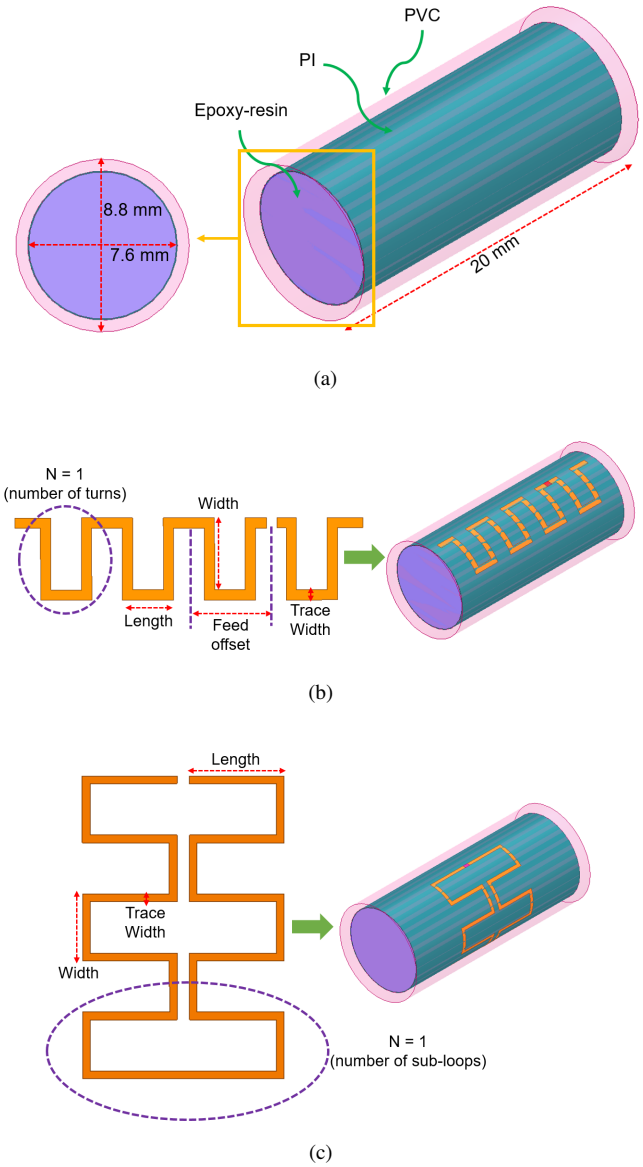

Fig. 2. The model of the capsule and the antennas and the parametrized dimensions (a) the model of the capsule (b) the model of the dipole antenna and the parametrized dimensions (c) the model of the loop antenna and the parametrized dimensions.

intestine, and the large intestine (Table I). These phantoms have the same physical and geometrical properties as the time-averaged GI phantoms. Fig. 3 shows the simulation results in 3 different GI tissue phantoms and in the time-averaged GI phantoms for all designs. From the results, it can be seen that the antennas operate in their intended frequency bands in any GI tissue. The maximum shift in the resonant frequency from the time-averaged GI phantom case is 7 MHz which is observed in the dipole antenna placed in the large intestine phantom at 434 MHz (straight green line and dashed red line in Fig. 3a). These results can be accounted for by the presence of the PVC layer. The PVC layer prevents the antennas from detuning during the transition through the GI tract as most of the fields created by the antennas are contained in this layer. The results indicate that the robustness of the ingestible antennas against the changes in the surrounding environment can be achieved with a proper choice of encapsulation. Therefore, it can be emphasized that an ingestible antenna designer would rather focus on methods to improve other parameters of the antenna such as efficiency rather than robustness. However, it must be noted that this work uses simplified homogeneous phantoms and does not take into account the air pockets that are likely to exist in a physical GI tract. Although the results obtained in this work provide the designers with an insight into the robustness of the ingestible antennas in the presence of the encapsulation layer, they are preliminary results and hence open to further investigation with more realistic models.

V. Conclusion

This paper examined the degree of possible detuning that may be encountered in the operation of ingestible antennas during the transition through different tissues in the GI tract. A meandered dipole antenna and a meandered loop antenna that are wrapped around a capsule covered with an encapsulation layer are optimized in spherical homogeneous time-averaged GI phantoms for 3 different frequencies. The results show that the considered ingestible antennas are robust against the changes in the EM properties of the GI tract due to the presence of the encapsulation layer. Our ongoing work aims at the fabrication and characterization of the developed antennas in liquid tissue-equivalent models. The results of these measurements will be presented during the conference.

Acknowledgment

This study was supported in part by the Région Bretagne through the project SAD “EM-NEURO” and in part by SATT Ouest Valorisation through the project “E-MOTION”.

References

[1] A. Kiourti and K. S. Nikita, “A review of in-body biotelemetry devices: Implantables, ingestibles, and injectables,” *IEEE Trans. Biomed. Eng.*, vol. 64, no. 7, pp. 1422–1430, 2017, doi: 10.1109/TBME.2017.2668612.

[2] H. Rajagopalan and Y. Rahmat-Samii, “Wireless medical telemetry characterization for ingestible capsule antenna designs,” *IEEE Antenn. Wireless Propag. Lett.*, vol. 11, pp. 1679–1682, 2012, doi: 10.1109/LAWP.2013.2238502.

[3] M. R. Yuce and T. Dissanayake, “Easy-to-swallow wireless telemetry,” *IEEE Microw. Mag.*, vol. 13, no. 6, pp. 90–101, 2012, doi: 10.1109/MMM.2012.2205833.

[4] J. Faerber, *et al.*, “In vivo characterization of a wireless telemetry module for a capsule endoscopy system utilizing a conformal antenna,” *IEEE Trans. on Biomed. Circuits Syst.*, vol. 12, no. 1, pp. 95–105, 2018, doi: 10.1109/TBCAS.2017.2759254.

[5] D. Nikolayev, M. Zhadobov, L. Le Coq, P. Karban, and R. Sauleau, “Robust ultraminiature capsule antenna for ingestible and implantable applications,” *IEEE Trans. Antennas Propag.*, vol. 65, no. 11, pp. 6107–6119, 2017, doi: 10.1109/TAP.2017.2755764.

[6] F. El hatmi, M. Grzeskowiak, D. Delcroix, T. Alves, S. Protat, S. Mostarshedi, and O. Picon, “A multilayered coil antenna for ingestible capsule: Near-field magnetic induction link,” *IEEE Antenn. Wireless Propag. Lett.*, vol. 12, pp. 1118–1121, 2013, doi: 10.1109/LAWP.2013.2270942.

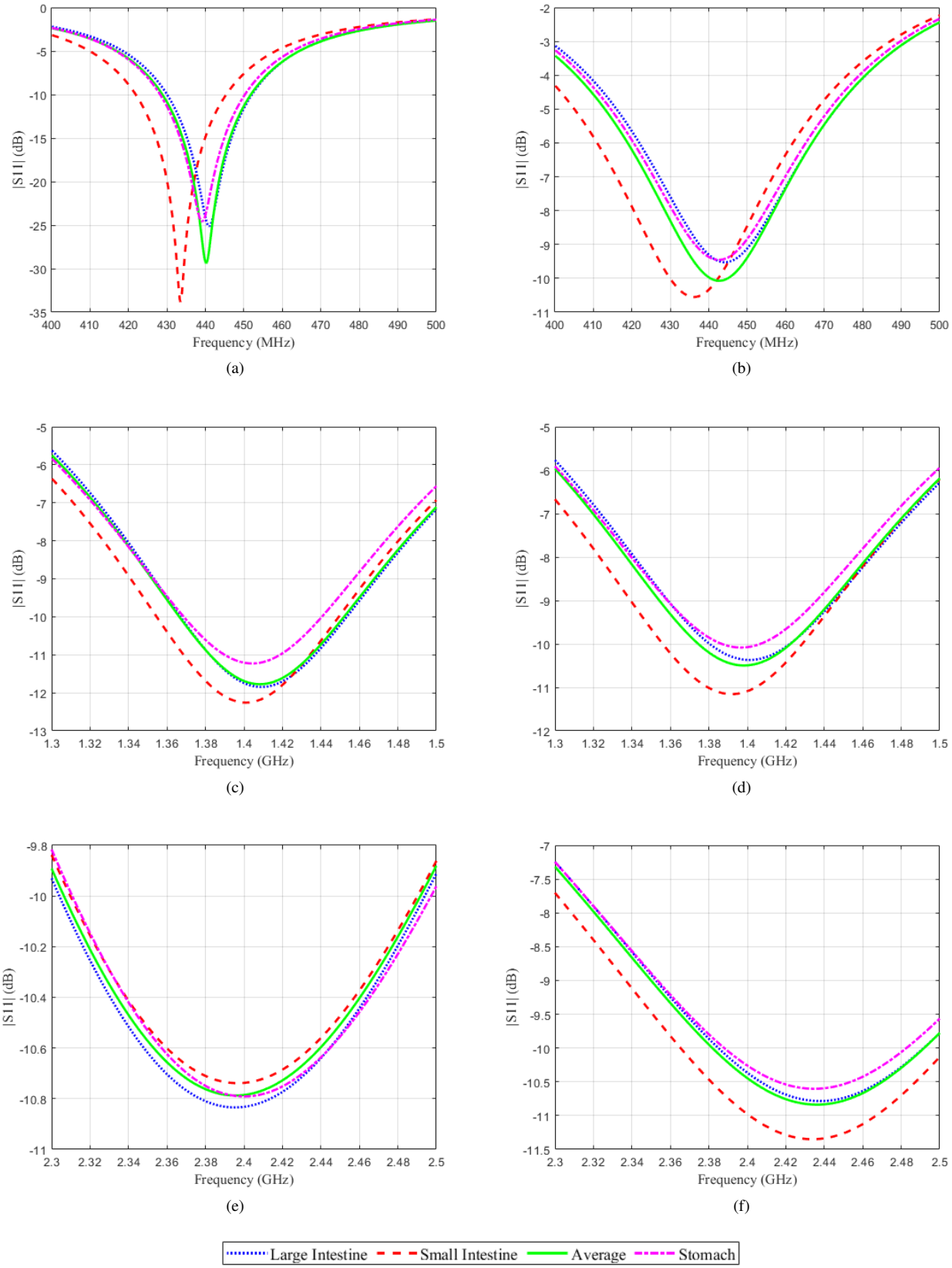

Fig. 3. The simulation results for the dipole and the loop antenna in 3 different GI tissue phantoms and in the time-averaged GI phantoms (a) results for the dipole at 434 MHz (b) results for the loop at 434 MHz (c) results for the dipole at 1.4 GHz (d) results for the loop at 1.4 GHz (e) results for the dipole at 2.4 GHz (f) results for the loop at 2.4 GHz.

[7] K. Kwon, W. Seo, S. Lee, and J. Choi, "Design of an antenna for an ingestible capsule endoscope system," in *Proc. 3rd Int. Conf. Netw. Infrastructure Digit. Content (IC-NIDC 2012)*, Beijing, China, 2012, pp. 62–65.

[8] S. Gabriel, R. W. Lau, and C. Gabriel "The dielectric properties of biological tissues: II. Measurements in the frequency range 10 Hz to 20 GHz," *Phys. Med. Biol.*, vol. 41, pp. 2251–2269, 1996.

[9] M. Bosiljevac, A. K. Skrivervik, and Z. Sipus, "In-body antennas design based on fundamental limits of obtainable power density," in *Proc. 15th Eur. Conf. Antennas Propag. (EuCAP 2021)*, Düsseldorf, Germany, 2021, pp. 1–5.

[10] D. Nikolayev, W. Joseph, M. Zhadobov, R. Sauleau, and L. Martens, "Optimal radiation of body-implanted capsules," *Phys. Rev. Lett.*, vol. 122, p. 108101, 2019.

[11] A. W. Damaj, H. M. El Misilmani, and S. A. Chahine, "Implantable antennas for biomedical applications: An overview on alternative antenna design methods and challenges," in *Proc. Int. Conf. High Performance Computing Simulation (HPCS 2018)*, Orleans, France, 2018, pp. 31–37.

[12] D. Nikolayev, M. Zhadobov, R. Sauleau, and P. Karban, "Antennas for ingestible capsule telemetry", in *Advances in Body-Centric Wireless Communication: Applications and State-of-the-Art.* London, U.K.: IET, 2016, pp. 143–186.

[13] S. S. Rao *et al.*, "Investigation of colonic and whole-gut transit with wireless motility capsule and radiopaque markers in constipation," *Clinical gastroenterology and hepatology*, vol. 7, no. 5, pp. 537–544, 2009.

[14] *IT'IS Foundation Dielectric Properties Table*, Oct. 2021. [Online]. Available: https://itis.swiss/virtual-population/tissue-properties/database/dielectric-properties/.

[15] D. Nikolayev, M. Zhadobov, and R. Sauleau, "Immune-to-detuning wireless in-body platform for versatile biotelemetry applications," *IEEE Trans. Biomed. Circuits Syst.*, vol. 13, no. 2, pp. 403–412, 2019, doi: 10.1109/TBCAS.2019.2892330.

[16] *ANSYS High Frequency Structure Simulator (HFSS)*, Oct. 2021. [Online]. Available: https://www.ansys.com/products/electronics/ansys-hfss.

[17] O. O. Olaode, W. D. Palmer, and W. T. Joines, "Effects of meandering on dipole antenna resonant frequency," *IEEE Antenn. Wireless Propag. Lett.*, vol. 11, pp. 122–125, 2012, doi: 10.1109/LAWP.2012.2184255.